

Bayesian Power Spectrum Analysis of the First-Year *WMAP* data

I. J. O’Dwyer¹, H. K. Eriksen^{2,3,4,5}, B. D. Wandelt^{1,6}, J. B. Jewell⁴, D. L. Larson⁶, K. M. Górski^{4,5,7}, A. J. Banday⁸, S. Levin⁴, P. B. Lilje²

ABSTRACT

We present the first results from a Bayesian analysis of the *WMAP* first year data using a Gibbs sampling technique. Using two independent, parallel supercomputer codes we analyze the *WMAP* Q, V and W bands. The analysis results in a full probabilistic description of the information the *WMAP* data set contains about the power spectrum and the all-sky map of the cosmic microwave background anisotropies. We present the complete probability distributions for each C_ℓ including any non-Gaussianities of the power spectrum likelihood. While we find good overall agreement with the previously published *WMAP* spectrum, our analysis uncovers discrepancies in the power spectrum estimates at low ℓ multipoles. For example we claim the best-fit Λ CDM model is consistent with the C_2 inferred from our combined Q+V+W analysis with a 10% probability of an even larger theoretical C_2 . Based on our exact analysis we can therefore attribute the "low quadrupole issue" to a statistical fluctuation.

Subject headings: cosmic microwave background — cosmology: observations — methods: numerical

¹Astronomy Department, University of Illinois at Urbana-Champaign, IL 61801-3080

²Institute of Theoretical Astrophysics, University of Oslo, P.O. Box 1029 Blindern, N-0315 Oslo, Norway

³Centre of Mathematics for Applications, University of Oslo, P.O. Box 1053 Blindern, N-0316 Oslo

⁴JPL, M/S 169/327, 4800 Oak Grove Drive, Pasadena CA 91109

⁵California Institute of Technology, Pasadena, CA 91125

⁶Department of Physics, University of Illinois at Urbana-Champaign, IL 61801-3080

⁷Warsaw University Observatory, Aleje Ujazdowskie 4, 00-478 Warszawa, Poland

⁸Max-Planck-Institut für Astrophysik, Karl-Schwarzschild-Str. 1, Postfach 1317, D-85741 Garching bei München, Germany

1. Introduction

Cosmic Microwave Background (CMB) power spectrum estimation from large datasets such as the Wilkinson Microwave Anisotropy Probe (*WMAP*) (Bennett *et al.* 2003a) presents a considerable computational challenge. With the exception of some specialized methods (Oh *et al.* 1999; Wandelt and Hansen 2003), obtaining the power spectrum and error bars for a generalized, large CMB dataset without introducing significant simplifications has, until now, been computationally impossible. However, a new numerical approach based on Gibbs sampling has been developed recently by Jewell, Levin, and Anderson (2004) and Wandelt, Larson, and Lakshminarayanan (2004) which offers the hope of overcoming these computational difficulties and allowing the analysis of large CMB datasets regardless of scanning strategy, noise characteristics and so on. In this letter we present our results from the application of this new method to the first year *WMAP* data. We developed two independent, parallel codes to achieve this and a detailed description of the implementation of these codes is given in a companion publication (Eriksen *et al.* 2004). The analysis results in a full, multivariate probabilistic description of the information the *WMAP* data set contains about the power spectrum and the all-sky map of the CMB anisotropies. For the purposes of this letter we limit ourselves to a presentation of the results at each angular scale ℓ , leaving a full multivariate exploration of the *WMAP* likelihood for a future publication. In §2 we give a very brief overview of our method and in §3 we present an overview of the implementation of our codes. §4 contains our results, provides some interpretation and discusses what light our method can shed on some of the anomalies in the *WMAP* power spectrum that have been discussed in the literature (e.g. Hinshaw *et al.* (2003); Spergel *et al.* (2003); Efstathiou (2004); Slosar, Seljak, & Makarov (2004)). Our conclusions and future directions for this work are detailed in §5.

2. Method Overview

In this section we present only a very brief overview of our method and codes and refer the reader to Eriksen *et al.* (2004) for a detailed discussion of our implementations and Jewell *et al.* (2004) and Wandelt *et al.* (2004) for a discussion of the underlying principles.

The main difference between our approach and previous attempts at power spectrum estimation is that rather than trying to solve the maximum likelihood problem directly, we *sample* from the probability density of the power spectrum C_ℓ given the data \mathbf{d} , $P(C_\ell|\mathbf{d})$. While directly sampling from this density is difficult or impossible, we can sample from the joint posterior density $P(C_\ell, \mathbf{s}|\mathbf{d})$, where \mathbf{s} is the CMB signal map. Expectation values of any statistic of the C_ℓ will converge to the expectation values of $P(C_\ell|\mathbf{d})$. The theory of

Gibbs sampling (Gelfand and Smith 1990; Tanner 1996) tells us that if we can sample from the conditional densities $P(\mathbf{s}|C_\ell, \mathbf{d})$ and $P(C_\ell|\mathbf{s}, \mathbf{d})$ then iterating the following two sampling equations will, after an initial burn-in period, lead to a sample from the joint posterior $P(C_\ell, \mathbf{s}|\mathbf{d})$:

$$\mathbf{s}^{i+1} \leftarrow P(\mathbf{s}|C_\ell^i, \mathbf{d}), \quad (1)$$

$$C_\ell^{i+1} \leftarrow P(C_\ell|\mathbf{s}^{i+1}). \quad (2)$$

Here the symbol “ \leftarrow ” denotes drawing a random realization from the density on the right. The conditional density of the signal given the most recent C_ℓ sample is $P(\mathbf{s}|C_\ell^i, \mathbf{d}) \propto G(S^i(S^i + N)^{-1}\mathbf{m}, ((S^i)^{-1} + N^{-1})^{-1})$, where \mathbf{m} is the map constructed from the data \mathbf{d} . To sample from this density we simply generate a Gaussian variate with the required mean and covariance. The density for the C_ℓ factorizes to an inverse gamma distribution due to the special form of S and sampling from this is very simple. For each ℓ we compute $\sigma_\ell = \sum_{m=-l}^{+l} |s_{lm}^i|^2$ and a $(2\ell-1)$ -vector of Gaussian random variates with zero mean and unit variance. Then $C_\ell^{i+1} = \frac{\sigma_\ell}{|\rho_\ell|^2}$. Given this sample from $P(C_\ell, \mathbf{s}|\mathbf{d})$, the marginalization over \mathbf{s} to obtain $P(C_\ell|\mathbf{d})$ is trivially accomplished: just ignore the \mathbf{s} in the tuple (C_ℓ, \mathbf{s}) . Of course this is not to say that the \mathbf{s} sample is purely ancillary in the analysis: it is also of interest to explore $P(\mathbf{s}|\mathbf{d})$ which is a full representation of the CMB signal content of the data.

The scaling of this Monte Carlo method is $\mathcal{O}(N_{\text{pix}}^{3/2})$ and corresponds to the scaling of the spherical harmonic transforms performed by the HEALPix algorithm. Other issues which affect our computational cost are the choice of a good preconditioner for our linear algebra solver, the correlation length between samples and the length of burn-in time required for the sampling scheme, eqs. 1 and 2, to converge. We perform the sampling in eq. 1, by means of solving linear systems of equations using the Conjugate Gradient algorithm. The computational cost of this method is therefore highly dependent on the choice of a good preconditioner for this system. We experimented with several preconditioners and found examples which gave convergence in a few tens of iterations. The number of samples we need to obtain in order to adequately describe the statistics of the power spectrum will depend upon the degree of correlation between successive samples. A detailed discussion of these issues can be found in Eriksen *et al.* (2004).

2.1. Foregrounds

An appealing feature of the sampling approach is its ability to incorporate virtually any real-world complications, as discussed by Jewell *et al.* (2004) and Wandelt *et al.* (2004). A few examples of this flexibility are applications to f^{-1} noise, asymmetric beams or arbitrary

sky coverage. Foreground estimation and removal are also possible. In principle, detailed prior knowledge of all anticipated foregrounds can be included and the algorithm will then return the level of the foreground supported by the data in the map. However, for this first analysis we limit ourselves to including two simple foreground components: (1) a stochastic model of the monopole and dipole in the maps, and (2) a stochastic model of the foreground component. These models are encoded in terms of uniform, improper priors that express our ignorance of the monopole and dipole in the maps as well as the foreground contributions in the regions that are flagged in the foreground masks supplied by the *WMAP* team. Traditionally this masked region is excluded from the analysis altogether. In the Bayesian approach it is modeled as a region where the foregrounds are completely unknown. Sampling from the posterior density reconstructs the signal in the masked region, based on the correlation structure discovered on the unmasked portion of the sky. The details of these foreground models are outlined in the above papers as well as in Eriksen *et al.* (2004).

3. Implementation

We used two independently developed implementations of the algorithm to produce our results: MAGIC (Wandelt 2004) and Commander. These are both parallel implementations of the sampling algorithm. Having results from both MAGIC and Commander allowed us to cross-check results and provided valuable redundancy. Our tests of the codes are detailed in Eriksen *et al.* (2004) and these showed that both codes were producing results consistent with each other. In both codes our noise model for each channel consisted of combining the published number of observations per pixel with the noise per sample for each channel and assuming the noise to be uncorrelated. We also show in Eriksen *et al.* (2004) that residual correlated noise in the *WMAP* maps has negligible effect on our results.

The data input to these codes were the first year *WMAP* maps¹ for all 8 of the cosmologically interesting frequency bands (2 at Q-, 2 at V- and 4 at W-band). For all channels we used template corrected maps following Bennett *et al.* (2003a). We performed two analyses with these data. First we analyzed the data in the V and W channels separately by band, using unweighted averages of the channel maps and computing an effective beam window function. For these runs we chose the conservative Kp0 mask and ran single, long chains, containing 1000 samples for each band. Q-band was analyzed more aggressively, combining the channels on the likelihood level (Eriksen *et al.* 2004), and using the Kp2 mask to assess potential foreground contamination. These analyses will be labeled Q, V and W in the

¹available at <http://lambda.gsfc.nasa.gov>

following.

The second analysis uses the optimal combination of all 8 channels in the likelihood using their respective noise specifications and beam window functions. We will refer to this joint analysis as QVW in the following. As before, we specified a stochastic model for the monopole and dipole component as well as complete ignorance about the foregrounds within a region on the sky. For the QVW analysis this region was defined by the more aggressive Kp2 mask. Both the Q and QVW analyses were done in parallel, short chains (~ 10 chains, ~ 100 samples each) initialized with plausible starting spectra inspired by the *WMAP* analysis (Hinshaw *et al.* 2003).

4. Results

All of the results presented here are based on ~ 1000 samples for each frequency band, which required a total of $\sim 15,000$ hours of CPU time

Figure 1 shows the Bayes estimate (posterior mean) for the signal QVW analysis. This map represents the CMB signal content in the Q, V, and W bands of the *WMAP* data. This map shows detail where the data warrants it and smoothes where the data is poor. The CMB signal is clearly visible outside the Galaxy and the algorithm has reconstructed the signal in the Galactic plane for the largest scale modes, consistent with the signal phases and correlations it has discovered on the high latitude sky. There is insufficient information in the map for the algorithm to reconstruct the smaller scale modes in the galactic plane. This result is a non-linear generalization of the Wiener filter which does not assume prior information about the signal correlations but discovers them from the data.

Figure 2 shows the power spectra we obtain for Q-, V- and W-band and the combined QVW analysis. Large scale features in the power spectra are consistently reproduced across all the channels.

In Figure 3, we show the probability distribution of the C_ℓ samples for some ℓ of interest. Since the original *WMAP* analysis was released there has been some controversy regarding a lack of power at the largest angular scales (lowest ℓ 's) e.g. (Efstathiou 2004; Slosar, Seljak, & Makarov 2004). It can be seen from the plots that our estimates of these C_ℓ 's are consistent with the original determinations made by the *WMAP* team, but that there are significant, non-Gaussian uncertainties on our estimates which indicate that low values of C_ℓ for the largest angular scales are not so unexpected. We also over-plot the results using the *WMAP* internal linear combination map with the Kp2 mask from Efstathiou (2004) in our figure. It can be seen that there is good agreement between the values obtained in our analysis and

that of Efstathiou.

For easy reference we show the cumulative probability distributions for the lowest ℓ in Figure 4. One can read off the probability that the actual theory C_ℓ are lower than the prediction from any particular model. Probabilities close to 0 or 1 indicate a poor fit, or outlier. A search over all strongly signal dominated ℓ from 2 to 350 using our V and W band analyses resulted in 10 outliers (within 0.01 of 0 or 1) for V band ($\ell = 54, 73, 114, 117, 121, 179, 181, 209, 300, 322$) and 9 outliers for W band ($\ell = 73, 82, 117, 121, 181, 261, 334, 341, 344$). For 349 tests this corresponds to only a slightly higher number of outliers than expected based on counting statistics, and is entirely unremarkable if we only count those outliers that appear in both bands. Based on this ℓ -by- ℓ analysis the “bite” in the spectrum does not seem particularly extraordinary, with only one outlier in the range of 200–220. However, all C_ℓ at $205 < \ell < 210$ are quite far below the best fit and will most likely be noted as a highly significant outlier in a full multivariate analysis of the joint posterior density.

5. Discussions and Conclusions

We have implemented the Gibbs sampling technique introduced by Jewell *et al.* (2004) and Wandelt *et al.* (2004), and applied it to the *WMAP* data. This first presentation of our results focuses on the inferred marginalized likelihoods for each ℓ . We find that these are broadly consistent with previous determinations of the power spectrum. By virtue of using a Bayesian analysis we can present a more complete picture of the uncertainties in the estimates across all relevant scales. Previous likelihood-based work to generate a full probabilistic description (e.g. Slosar, Seljak, & Makarov (2004)) were limited to looking at only the lowest ℓ due to the computational difficulty involved. We present an analysis that covers the region from $\ell = 2$ to $\ell = 500$. A multivariate treatment will therefore allow a rigorous assessment of the significance of anomalies in the power spectrum such as the low power on large angular scales, the “bite” in the power spectrum near the peak, etc., as well as using the full multivariate posterior density as the input to parameter estimation. This is particularly interesting since the Bayesian approach yields a *converging* analytic approximation to the likelihood of C_ℓ given the data, it is not necessary to construct parametric approximations to the likelihood such as the Gaussian or shifted log-normal approximations. A detailed study of these issues will be presented in a future publication.

More information can be drawn from the data in the future. The extension to more complex foreground models, the inclusion of correlated noise and the addition of polarization to the analysis will all be of great interest, especially in view of the upcoming release of the

second year of *WMAP* data and, further in the future, the *Planck* experiment.

We acknowledge use of the HEALPix² software (Górski, Hivon & Wandelt 1998) and analysis package. We also acknowledge use of the Legacy Archive for Microwave Background Data Analysis (LAMBDA). H. K. E. and P. B. L. acknowledge financial support from the Research Council of Norway, including a Ph. D. studentship for H. K. E. This work has also received support from The Research Council of Norway (Programme for Supercomputing) through a grant of computing time. This work was partially performed at the Jet Propulsion Laboratory, California Institute of Technology, under a contract with the National Aeronautics and Space Administration. This work was partially supported by an NCSA Faculty Fellowship for B.D.W. This research used resources of the National Energy Research Scientific Computing Center, which is supported by the Office of Science of the U.S. Department of Energy under Contract No. DE-AC03-76SF00098.

REFERENCES

- Bennett, C. L. *et al.* 2003a, *ApJS*, 148, 1
- Bennett, C. L. *et al.* 2003b, *ApJS*, 148, 97
- Efstathiou, G. 2004, *MNRAS*, 348, 885
- Eriksen, H. K. *et al.* 2004, *ApJS*, accepted, astro-ph/0407028
- Gelfand, A. E. and Smith, A. F. M. 1990, *J. Am. Stat. Asso.* 85, 398
- Górski, K. M., Hivon, E., & Wandelt, B. D., 1999, in *Evolution of Large-Scale Structure: from Recombination to Garching*, ed. A. J. Banday, R. K. Sheth, & L. N. da Costa (Garching, Germany: European Southern Observatory), 37
- Hinshaw, G. *et al.* 2003, *ApJS*, 148, 135
- Jewell, J., Levin, S., & Anderson, C. H. 2004, *ApJ*, 609, 1
- Oh, S. P., Spergel, D. N., & Hinshaw, G. 1999, *ApJ*, 510, 551
- Slosar, A., Seljak, U., & Makarov, A. 2004, *Phys. Rev. D*, 69, 123003

²<http://www.eso.org/science/healpix/>

Spergel, D. N., *et al.*, 2003 ApJS, 148, 175S

Tanner, M. A. 1996, *Tools for statistical inference*, 3rd e. Springer-Verlag, New York.

Wandelt, B. D., Larson, D. L., & Lakshminarayanan, A. 2003, PRD accepted [astro-ph/0310080]

Wandelt, B. D. 2004, in “Stanford 2003, Statistical problems in particle physics, astrophysics and cosmology”, Lyons, L. *et al.* (Eds.), p. 229 [astro-ph/0401623]

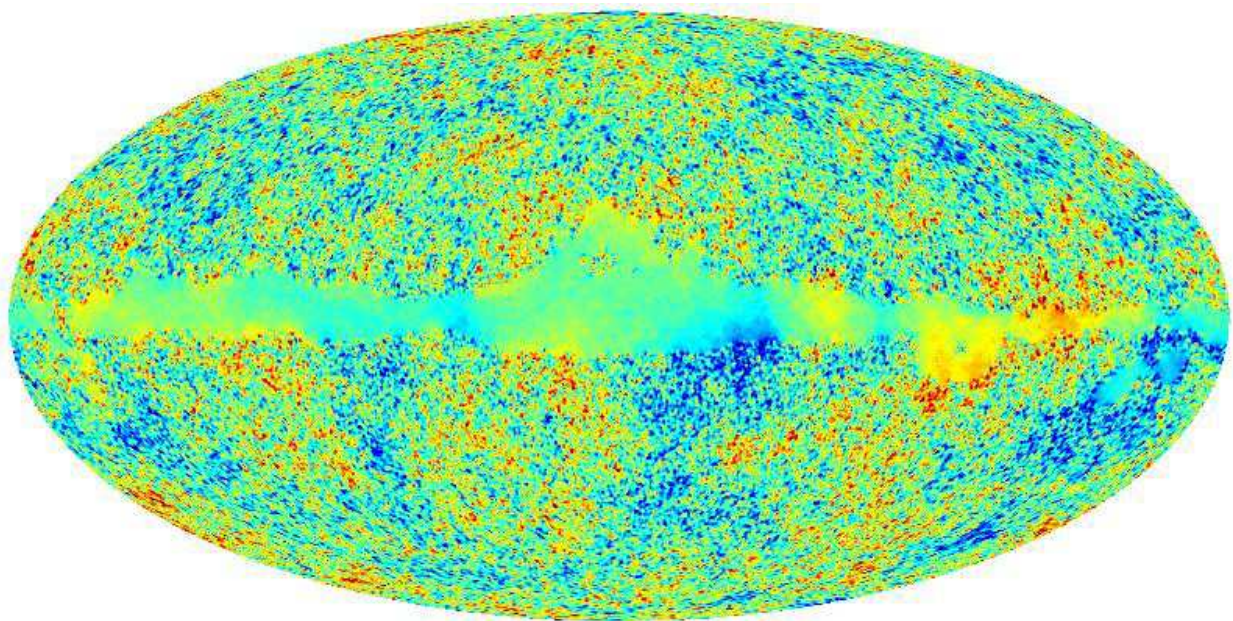
Wandelt, B. D. and Hansen, F. 2003, Phys. Rev. D, 67, 023001

Fig. 1.— The posterior mean $\langle \mathbf{s} \rangle_{P(\mathbf{s}|\mathbf{d})}$ of the CMB signal \mathbf{s} given the *WMAP* first year data, including all 8 channels in the Q, V and W bands. This map represents the CMB signal content of the *WMAP* data. It contains detail where the data warrants it and smoothes where the data is poor. For example, the algorithm is able to reconstruct the largest scale modes in the Galactic plane based on the signal phases and correlations it discovers in regions of the map outside the Galactic plane. The smallest scale which can be reproduced in the Galactic plane is set by the mask size and is a natural consequence of Wiener filtering.

Fig. 2.— Four power spectra obtained from the Gibbs sampling algorithm. The uppermost panel shows the Q-band power spectrum, then V-band, W-band and finally the lower panel the combined analysis from all eight cosmologically interesting *WMAP* channels. Gray dots represent the individual samples and the dark line is the mode of the unbinned power spectrum. The lighter gray line in the bottom panel is the *WMAP* combined CMB power spectrum and where the line is not visible the difference between our result and the original *WMAP* result differ by less than the width of the line. The Q and Q+V+W result was obtained with an initial power spectrum based on the *WMAP* best-fit power spectrum with a random component, while the V and W results were obtained using an initial spectrum proportional to $1/\ell(\ell + 1)$. Our V and W results were obtained using the conservative Kp0 mask while our Q-band result uses the Kp2 mask. This was done to assess potential foreground contamination, which we find no evidence for.

Fig. 3.— The probability distributions of the C_ℓ samples for a selected set of ℓ giving the probability of obtaining a value of C_ℓ within a given histogram bin. We plot results for the significantly non-Gaussian low- ℓ multipoles and for selected higher values based on their deviation from the best-fit Λ -CDM model. There are 50 bins in each histogram. Red, green and blue histograms are Q, V and W-band respectively. Black is the combined QVW analysis. The dotted vertical line is the *WMAP* best estimate of the C_ℓ value. The solid line is the *WMAP* best fit theory C_ℓ 's and the dash-dot-dot line is the average of the samples from our algorithms. For $\ell < 7$ the dashed lines show the *WMAP*-ILC values from Efstathiou (2004) for comparison. Further plots are available at <http://www.astro.uiuc.edu/~iodwyer/research#wmap>.

Fig. 4.— Easy-to-use representation for evaluating theoretical models of the power spectrum at the lowest ℓ . We plot the probability $P(C_\ell^{\text{theory}} < C_\ell)$ against $\ell(\ell + 1)C_\ell/2\pi$ for the largest angular scales probed by *WMAP*. Theorists can evaluate the goodness of fit of their model C_ℓ with the *WMAP* data by reading off the probability from this graph. If P is within 0.025 of 1 or 0, the model would be ruled out at the 5% level based on that ℓ alone. The vertical dotted line is the *WMAP* best fit theory assuming a constant scalar spectral index n_s . The probability is $\sim 90\%$ that the the actual theory C_2 is smaller.



-300 μK  300 μK

